

Synthesis and Characterization of Monodisperse Core–Shell Colloidal Spheres of Zinc Sulfide and Silica

Krassimir P. Velikov^{*,†} and Alfons van Blaaderen^{*,†,‡}

Condensed Matter Department, Debye Institute, Utrecht University, Ornstein Laboratory, Princetonplein 1, 3584 CC Utrecht, The Netherlands, and FOM Institute for Atomic and Molecular Physics, Kruislaan 407, 1098 SJ Amsterdam, The Netherlands

Received January 30, 2001. In Final Form: May 11, 2001

We report on a new type of composite particles consisting of a zinc sulfide (ZnS) core and a silica (SiO₂) shell or vice versa. We developed and optimized these particles for photonic applications, because ZnS has a large refractive index and does not absorb light in the visible and both ZnS and SiO₂ can be easily doped with fluorophores. Both kinds of morphologies were created using a seeded growth procedure using monodisperse seeds on which homogeneous layers with a well-defined thickness were grown. Moreover, the ZnS and SiO₂ cores could be completely dissolved leaving SiO₂ and ZnS shells, respectively, filled with solvent or air after drying. The particle morphology was investigated by electron microscopy. The optical properties were studied by extinction measurements and angle resolved light scattering and compared to scattering theory.

Introduction

Recently, a lot of interest in core–shell colloidal particles has arisen from the ability to fine-tune their properties. The structure, size, and composition of these particles can be easily altered in a controllable way to tailor their magnetic, optical, mechanical, thermal, electrical, electro-optical, and catalytic properties.^{1–7} Core–shell particles with a shell optically matched to the suspending fluid can be employed as a model system to study direct particle–particle interactions in a fluid or a colloidal crystal.⁸ The core–shell morphology can be used as a precursor form to produce hollow spheres⁹ or to lower the cost of precious materials by coating them on inexpensive cores.^{10,11}

An exciting area of application of colloidal particles is that of photonic band gap materials.^{12–14} These materials can be used for the manipulation of light propagation and spontaneous emission.^{15–17} Colloids are ideal building

blocks for the creation of photonic crystals, because of their ability to self-organize in three-dimensional (3D) periodic structures with different symmetries. Core–shell particles consisting of high-index core (e.g., ZnS) and low-index shell (e.g., SiO₂) or vice versa are of special interest.¹³ By changing the thickness of the shell with respect to the core, one can tune the filling fraction of the components and control the optical properties. Further, the cores can be dissolved to obtain a crystal or single particles of hollow shells of high- or low-index material.

Zinc sulfide (ZnS) is a widely used metal sulfide with many technological applications (e.g., as a pigment¹⁸ or in electroluminescence panels,¹⁹ infrared-windows,²⁰ and solar cells²¹). ZnS colloidal particles of different size and low polydispersity can be obtained by a homogeneous precipitation and aggregation process.^{22–25} Because of the high bulk refractive index ($n \sim 2.36$ ($\lambda = 589$ nm) for cubic β -ZnS) and lack of absorption in the visible,²⁶ ZnS is an appropriate material for photonic applications, such as optical cavities and photonic crystals. Moreover, ZnS can be doped, for example, with manganese,²⁷ to induce luminescence, or a fluorescent dye can be incorporated into the silica layer at a well-defined radial position.²⁸ Recent theoretical calculations have shown that a face-cubic-centered (fcc) colloidal crystal of ZnS core–SiO₂ shell particles with a suitable shell thickness has a larger relative L-stopgap in comparison to a crystal of homo-

* Corresponding authors. E-mails: K.P.Velikov@phys.uu.nl and A.vanBlaaderen@phys.uu.nl.

[†] Utrecht University.

[‡] FOM Institute for Atomic and Molecular Physics.

(1) Phillipse, A. P.; van Bruggen, M. P. B.; Pathmamanoharan, C. *Langmuir* **1994**, *10*, 92.

(2) Caruso, F.; Susha, A. S.; Giersig, M.; Mohwald, H. *Adv. Mater.* **1999**, *11*, 950.

(3) Chang, S. Y.; Liu, L.; Asher, S. A. *J. Am. Chem. Soc.* **1994**, *116*, 6739.

(4) Giersig, M.; Ung, T.; Liz-Marzan, L. M.; Mulvaney, P. *Adv. Mater.* **1997**, *9*, 570.

(5) Ung, T.; Liz-Marzan, L. M.; Mulvaney, P. *Langmuir* **1998**, *14*, 3740.

(6) Oldenburg, S. J.; Averitt, R. D.; Westcott, S. L.; Halas, N. J. *Chem. Phys. Lett.* **1998**, *288*, 243.

(7) Averitt, R. D.; Sarkar, D.; Halas, N. J. *Phys. Rev. Lett.* **1997**, *78*, 4217.

(8) Viravathana, P.; Marr, D. W. M. *J. Colloid Interface Sci.* **2000**, *221*, 301.

(9) Zhong, Z. Y.; Yin, Y. D.; Gates, B.; Xia, Y. N. *Adv. Mater.* **2000**, *12*, 206.

(10) Ocana, M.; Hsu, W. P.; Matijevic, E. *Langmuir* **1991**, *7*, 2911.

(11) Hsu, W. P.; Yu, R. C.; Matijevic, E. *J. Colloid Interface Sci.* **1993**, *156*, 56.

(12) Soukoulis, C. M. *Photonic Crystals and Light Localization*; Kluwer Academic Publishers: Dordrecht, 2000; Vol. 315.

(13) van Blaaderen, A. *MRS Bull.* **1998**, *23*, 39.

(14) Soukoulis, C. M. *Photonic Band Gap Materials*; Kluwer Academic Publishers: Dordrecht, 1996.

(15) Yablonovitch, E. *Phys. Rev. Lett.* **1987**, *58*, 2059.

(16) Bykov, V. P. *Sov. J. Quantum Electron.* **1975**, *4*, 861.

(17) John, S. *Phys. Rev. Lett.* **1987**, *58*, 2486.

(18) Scholz, S. M.; Vacassy, R.; Dutta, J.; Hofmann, H.; Akinc, M. *J. Appl. Phys.* **1998**, *83*, 7860.

(19) Mach, R.; Muller, G. O. *J. Cryst. Growth* **1988**, *86*, 866.

(20) Harris, D. C. *Infrared Phys. Technol.* **1998**, *39*, 185.

(21) Yamaguchi, T.; Yamamoto, Y.; Tanaka, T.; Yoshida, A. *Thin Solid Films* **1999**, *344*, 516.

(22) Wilhelmly, D. M.; Matijevic, E. *J. Chem. Soc., Faraday Trans.* **1984**, *80*, 563.

(23) Williams, R.; Yocum, P. N.; Sofko, F. S. *J. Colloid Interface Sci.* **1985**, *106*, 388.

(24) Celikkaya, A.; Akinc, M. *J. Am. Ceram. Soc.* **1990**, *73*, 245.

(25) Celikkaya, A.; Akinc, M. *J. Am. Ceram. Soc.* **1990**, *73*, 2360.

(26) Palik, E. *Handbook of Optical Constants of Solids*; Academic Press: San Diego, CA, 1997.

(27) Bhargava, R. N.; Gallagher, D.; Hong, X.; Nurmikko, A. *Phys. Rev. Lett.* **1994**, *72*, 416.

(28) van Blaaderen, A.; Vrij, A. *Langmuir* **1992**, *8*, 2921.

geneous ZnS or SiO₂ spheres.²⁹ In addition, the relative L-stopgap is also larger than in the case of a crystal from SiO₂ core–ZnS shell particles or even hollow ZnS shells.³⁰

Coating of colloidal particles with a silica layer has many advantages, because such a shell is chemically inert and optically transparent. Furthermore, the colloid chemistry of silica is well understood,³¹ and many possibilities for surface modification are available. Finally, coating by silica in a seeded growth process^{32–34} leads to a decrease in the polydispersity of the particles and reduces the van der Waals attraction, which enhances the colloid stability and ability to form colloidal crystals. A silica coating has already been applied to CdS³⁵ and ZnS³⁶ semiconductor nanocrystals and metal,^{5,37–42} inorganic,^{8,43} and polymer⁴⁴ colloidal particles. The thin silica layer increases the mechanical stability, makes possible a transfer into organic solvents, provides for a capping layer on the semiconductor nanocrystals, and protects metal particles against oxidation. Finally, we recently invented a way to turn the spherical SiO₂ and ZnS particles into ellipsoidal particles by ion irradiation.⁴⁵

In the present work, we will describe the coating of ZnS colloidal particles of different sizes with a SiO₂ layer and vice versa using seeded growth procedures. ZnS and SiO₂ cores were completely dissolved leaving SiO₂ and ZnS shells, respectively, filled with solvent. The optical properties of the particles were studied by means of static light scattering (SLS) and extinction measurements and compared with scattering theory.

Experimental Section

Materials. Zn(NO₃)₂·4H₂O, ammonia (30 wt % NH₃), and nitric acid of analytical reagent quality were purchased from Merck, fluorescein–isothiocyanate (FITC, isomer I) was purchased from Sigma, and thioacetamide (TAA), hydrofluoric acid (HF), and tetraethoxysilane (TES) of puriss grade quality were obtained from Fluka. Absolute technical grade ethanol (Nedalc) or analytical grade ethanol (Merck) and Milli-Q water were used in all preparations. All solvents and chemicals were used as received.

Particle Characterization. Transmission electron microscopy (TEM) and scanning electron microscopy (SEM) were carried out on Philips CM10 and Philips XL30 FEG microscopes, respectively. The relative width of the size distribution (the polydispersity δ) was determined by image processing; typically, around 200 particles were counted. SLS measurements on dilute suspensions in ethanol were performed on a Fica 50 or a

homemade light scattering apparatus. Extinction spectra were measured in ethanol using a Cary 100E UV–vis spectrophotometer. The optical path in the suspension was 1.00 cm. Suspensions were sufficiently diluted (<10^{−5} vol %) to avoid interactions between particles and to keep multiple scattering contributions negligible. Fitting of the spectra was performed using the computer algorithm developed by Bohren and Huffman,⁴⁶ adapted to take size polydispersity into account.

Silica Core Synthesis. Monodisperse SiO₂ particles were synthesized following the Stöber–Fink–Bohn procedure.⁴⁷ A fluorescent dye (FITC) was incorporated into the silica spheres as described by van Blaaderen et al.²⁸

ZnS Core Synthesis. Zinc sulfide colloidal particles of different sizes were obtained by homogeneous precipitation–aggregation from acidic zinc nitrate aqueous solutions using the thermal decomposition of TAA as a source of sulfide ions.^{22,24,25,48} Typical starting conditions used in our experiments were 0.001–0.05 M Zn²⁺, 0.01–0.10 M HNO₃, [Zn²⁺]/[TAA] = 4–10, and a constant temperature in the range of 60–70 °C. The TAA was first dissolved in water, and the solution was heated to the reaction temperature; then, a mixture of Zn(NO₃)₂ and HNO₃ solution was quickly added, and the reaction vessel was immersed in a water bath set at the reaction temperature. The precipitation reaction was carried out in two stages because this turned out to provide more monodisperse particles. In the first stage, a population of particles was obtained as described above and in the literature.^{22,24,25,48} However, in some experiments, following Wilhelmy and Matijevic,²² the solution was first kept at room temperature for 5 h and then placed in the water bath at an elevated temperature. After a certain period of aging, in which the primary particles reached the desired radius, the precipitation reaction was quenched by cooling the vessel in cold water (~15 °C) accompanied by vigorous agitation. The decrease in temperature and the mechanical agitation led to a secondary nucleation. In some cases, the first population of big particles was separated from the solution by centrifugation. The mother liquor with the second population of nuclei was placed again in the warm water bath, and the reaction continued, until the secondary particles reached the desired size. The final radius of the particles was controlled by the heating time, which ranged from 30 min to 3 h. The particles were separated from the mother liquid by centrifugation, washed twice with water, and redispersed in ethanol by ultrasonification. Suspensions were stored and remained stable in ethanol.

Coating of ZnS Cores with SiO₂. A direct coating of the ZnS particles with a silica layer was performed in two steps, based on a modification of the original Stöber method⁴⁷ to seeded growth.^{32–34} In the first step, concentrated ammonia (30 wt % NH₃) was added to a vigorously stirred ZnS suspension in ethanol (with a particle concentration n of ~10⁹ cm^{−3}) to a concentration of 0.10 M in NH₃. Subsequently, a certain amount of TES was added. Some of the experiments were performed with an additional amount of water added to a total concentration of 1.00 M. The amount of TES was calculated to cover the particle with a silica layer of thickness ~50 nm. Typically, when no additional amount of water was added the condensation of TES was slow and took more than 5 h.³⁴

In the second step, the ammonia concentration was increased to 0.60 M, and the water concentration was adjusted to 2.00 M. The TES was added in small portions, to prevent a secondary nucleation of pure silica particles.³² The final core–shell particles were separated by centrifugation, washed twice with ethanol, and then redispersed by ultrasonification in pure ethanol.

SiO₂ Shells. Hollow silica shells were obtained after dissolving the ZnS cores using a mineral acid. Typically, 0.001 M nitric acid was added to a dilute (<0.1 vol %) water (50 vol %)–ethanol (50 vol %) suspension of ZnS core–SiO₂ shell particles at moderate stirring. A higher acid concentration induced aggregation. For a ZnS core of radius ~125 nm, the dissolution process was carried out for 24 h. Depending on the core–shell particle morphology,

- (29) Moroz, A.; Sommers, C. *J. Phys.: Condens. Matter* **1999**, *11*, 997.
 (30) Moroz, A. Private communication, 2000.
 (31) Bergna, H. E. *The Colloid Chemistry of Silica*; American Chemical Society: Washington, DC, 1994; Vol. 234.
 (32) Philipse, A. P. *Colloid Polym. Sci.* **1988**, *266*, 1174.
 (33) Bogush, G. H.; Zukoski, C. F. *J. Colloid Interface Sci.* **1991**, *142*, 19.
 (34) van Blaaderen, A.; van Geest, J.; Vrij, A. *J. Colloid Interface Sci.* **1992**, *154*, 481.
 (35) Correa-Duarte, M. A.; Giersig, M.; Liz-Marzan, L. M. *Chem. Phys. Lett.* **1998**, *286*, 497.
 (36) Iler, R. K. U.S. Patent 2,885,366, 1959.
 (37) Ohmori, M.; Matijevic, E. *J. Colloid Interface Sci.* **1993**, *160*, 288.
 (38) Liz-Marzan, L. M.; Philipse, A. P. *J. Colloid Interface Sci.* **1995**, *176*, 459.
 (39) Alejandro-Arellano, M.; Ung, T.; Blanco, A.; Mulvaney, P.; Liz-Marzan, L. M. *Pure Appl. Chem.* **2000**, *72*, 257.
 (40) Mulvaney, P.; Liz-Marzan, L. M.; Giersig, M.; Ung, T. *J. Mater. Chem.* **2000**, *10*, 1259.
 (41) Yang, C. S.; Liu, Q.; Kauzlarich, S. M.; Phillips, B. *Chem. Mater.* **2000**, *12*, 983.
 (42) Hardikar, V. V.; Matijevic, E. *J. Colloid Interface Sci.* **2000**, *221*, 133.
 (43) Ohmori, M.; Matijevic, E. *J. Colloid Interface Sci.* **1992**, *150*, 594.
 (44) Goller, M. I.; Vincent, B. *Colloids Surf., A* **1998**, *142*, 281.
 (45) Snoeks, E.; van Blaaderen, A.; van Dillen, T.; van Kats, C. M.; Brongersma, M. L.; Polman, A. *Adv. Mater.* **2000**, *12*, 1511.

(46) Bohren, C. F.; Huffman, D. R. *Absorption and scattering of light by small particles*; Wiley: New York, 1983.

(47) Stöber, W.; Fink, A.; Bohn, E. *J. Colloid Interface Sci.* **1968**, *26*, 62.

(48) Vacassy, R.; Scholz, S. M.; Dutta, J.; Plummer, C. J. G.; Houriet, R.; Hofmann, H. *J. Am. Ceram. Soc.* **1998**, *81*, 2699.

Table 1. Radius (R) and Polydispersity (δ) of ZnS Cores Obtained after a Secondary or Primary Nucleation Burst (See Text) As Determined by TEM

sample code	R [nm]	δ %	nucleation burst
50SN	81	8	secondary
56SN	84	5	secondary
55SN	103	3	secondary
57SN	133	6	secondary
32	270	9	primary
54SN	346	6	secondary
61SN	818	7	secondary
13	1415	1	primary

SiO₂ shells filled with solvent or a silica replica of the pores in the ZnS cores was obtained.

Coating of SiO₂ Cores with ZnS. SiO₂ core–ZnS shell particles were obtained by homogeneous precipitation of ZnS onto silica seeds in water–ethanol solutions using the thermal decomposition of TAA as a source of sulfide ions. The same concentration range of Zn²⁺, HNO₃, and [Zn²⁺]/[TAA] ratio as for producing of the ZnS cores was used. An ethanol suspension of fluorescently labeled SiO₂ seeds of radius ~ 202 nm ($n \sim 10^{10}$ cm⁻³) was mixed with an equal volume of water containing the dissolved TAA. Then, the mixture of Zn²⁺ and HNO₃ was quickly added, and the reaction vessel was placed in a water bath at 60 °C. The reaction was carried out for 2–3 h at slow stirring. The final particles were separated by centrifugation, washed twice with ethanol, and then redispersed by ultrasonification in pure ethanol. As in the case of pure ZnS particles, suspensions were stored and remained stable in ethanol.

ZnS Shells. Solvent-filled ZnS shells were obtained after dissolving the SiO₂ cores using hydrofluoric acid. Typically, 1 wt % HF in water was added to a dilute (<0.1 vol %) suspension of SiO₂ core–ZnS shell particles in ethanol at moderate stirring. Silica cores were dissolved within ~ 5 min. The ZnS shells did not dissolve within the reaction time and remained as hollow shells.

Results and Discussion

ZnS Cores. By use of the above-described procedure, spherical ZnS particles with a narrow size distribution (<8%) were obtained. The final particle radius, depending on the reaction time and conditions, varied from 80 nm up to 1.4 μ m (Table 1). Examples of electron micrographs of ZnS cores demonstrating the range of sizes obtained with the method are shown in Figure 1. The particles were prepared using different experimental conditions, but in all cases the particle size was controlled through the reaction time. The mechanism of ZnS precipitation–aggregation and particle morphology are well understood.^{48,49} The ZnS particles are aggregates consisting of small (~ 10 nm) nanocrystals mainly of cubic β -ZnS. The crystalline structure and crystal size were inferred from X-ray diffraction measurements.^{24,49} Because of the aggregation mechanism, ZnS particles are porous and consist of ~ 50 –80% ZnS.¹⁸ The porosity and the average density depend on the particle size, and reaction conditions and light scattering results discussed below indicate that the larger particles do not have a homogeneous density distribution.

Polydispersity is an important parameter if colloidal particles are used as a model system to study crystallization, melting, or the glass transition.⁵⁰ In contrast to previously reported results,^{22,23} a significantly lower polydispersity was achieved without additional purification of the TAA. In general, the polydispersity was below 8%, but in some cases in which a low initial Zn²⁺

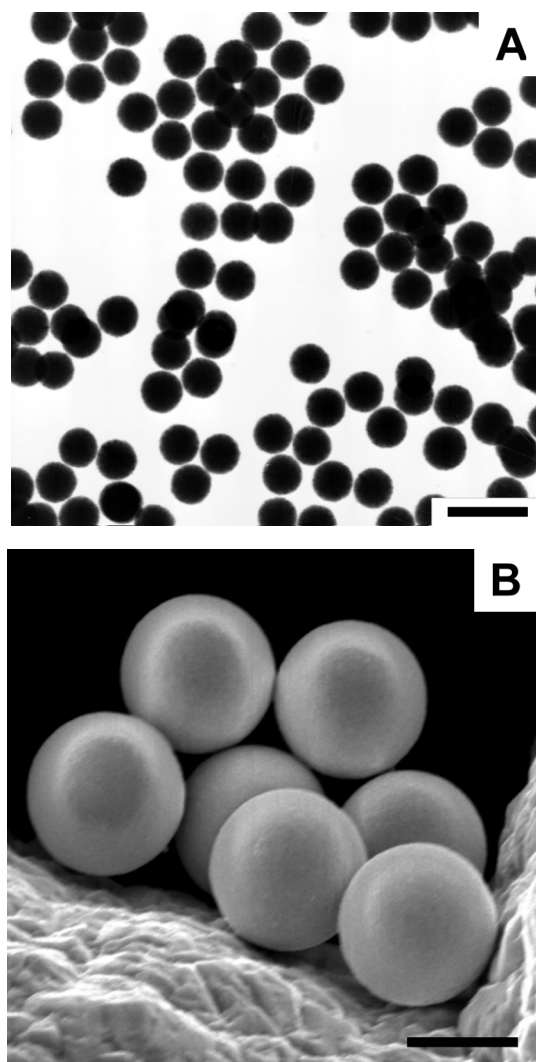


Figure 1. TEM (a) and SEM (b) micrographs of spherical monodisperse ZnS particles obtained through homogeneous precipitation–aggregation from aqueous solutions of zinc nitrate demonstrating the range of sizes possible: (a) sample 55SN, $R = 103$ nm, $\delta = 3\%$, scale bar 400 nm; (b) sample 13, $R = 1.414$ μ m, $\delta = 1\%$, scale bar 2 μ m. The size and polydispersity were determined by TEM.

concentration was used, a polydispersity of $\sim 1\%$ was reached (Figure 1b). The initial and the secondary nucleation influence the final size distribution of ZnS. The nucleation process is very sensitive to impurities and thermal or mechanical fluctuations. The secondary nucleation is caused by an excess of Zn²⁺ and S²⁻ ions, which were not consumed during the primary particle growth. The secondary particles were generally observed to have a lower polydispersity and higher concentration. A possible explanation is that the secondary nucleation takes place in a more homogeneous medium and at a higher concentration of S²⁻ in the solution. The higher concentration of sulfide ions in the solution leads to a higher concentration of nuclei. A secondary nucleation could both be induced by agitation or cooling the reaction vessel. Once generated, the secondary particles were further grown to a desired size. The main disadvantage of the method is the difficult control over the final particle size. However, by use of seeded growth (see below), this problem is overcome.

The stability of an aqueous ZnS suspension has been studied in detail,^{51,52} but to our knowledge no data are available on stability in organic solvents. It is our finding

(49) Scholz, S. M.; Vacassy, R.; Lemaire, L.; Dutta, J.; Hofmann, H. *Appl. Organomet. Chem.* **1998**, *12*, 327.

(50) Kegel, W. K.; van Blaaderen, A. *Science* **2000**, *287*, 290 and references therein.

Table 2. Radius (R) and Polydispersity (δ) of ZnS–SiO₂ Composite and ZnS Core–SiO₂ Shell Particles Obtained after a Seeded Coating of ZnS Cores with Silica As Determined by TEM

sample code	R [nm]	δ %	morphology ^a
56SN-S1	85	6	composite
56SN-S1-S	128	5	core–shell
57SN-S1	125	5	composite
50SN-S1	81	8	composite
50SN-S1-S	245	6	core–shell
50SN-S1-S1	338	4	core–shell
54SN-S3-S	351	5	core–shell

^a “Composite” means that the silica penetrates into the ZnS core.

that ZnS particles of any size form a stable suspension in ethanol, where they were kept before coating with silica.

ZnS Core–SiO₂ Shell. ZnS seeds were directly coated with a silica layer of the desired thickness by hydrolysis and condensation of TES in an ethanol–water–ammonia mixture. The most important factor in the coating process is the stability of the initial seed suspension at the reaction conditions. By use of a concentration of 0.10 M of ammonia, particles of different size were initially coated with a very thin silica layer without aggregation. Table 2 gives examples of coated ZnS cores with silica with different thickness and morphology. A ZnS colloidal suspension was found to be stable at 0.10 M NH₃ (0.22 M H₂O) in a water–ethanol–ammonia mixture; however, at higher concentrations of ammonia (used for seeded growth of pure silica spheres^{32,34}) the ZnS cores aggregated. At a pH higher than the isoelectric point (IEP = 7.2^{53,54}), ZnS is negatively charged because of the presence of HS[−] and negatively charged hydrolysis products on the particle surface. However, as we did not prevent the presence of oxygen, it is likely that the outside layer is composed of ZnO.^{51,52} In principle, this facilitates the growth of SiO₂ on the particle surface. As surface oxidation is quite common for many sulfides, this suggests that coating of large colloidal particles of metal sulfides with a silica layer is generally possible.

The deposited silica layer has a different morphology depending on the ZnS particle porosity and reaction conditions. If the particles are small and porous (<200 nm), the initial silica is first deposited inside the particle pores forming a ZnS–silica composite core (Figure 2). The very thin silica layer cannot be determined by TEM initially, but the light scattering experiments clearly show a change in the effective refractive index of the particles because of the presence of silica inside the pores without a significant change in size. However, after dissolving the ZnS the silica remains and can be directly imaged by TEM (see below). In this way, the silica can provide for mechanical stabilization of small and porous aggregates of metal sulfides. If the particles are bigger or the coating is performed at higher water concentration (higher hydrolysis rate of TES), silica cannot diffuse deep into the particle and quickly forms a layer leading to core–shell particles (Figure 3).

The conditions necessary to stabilize the ZnS suspension are not optimal to grow silica.^{32,34} For this reason, the ammonia concentration was increased to 0.6 M only after the first thin silica layer was deposited. At this ammonia

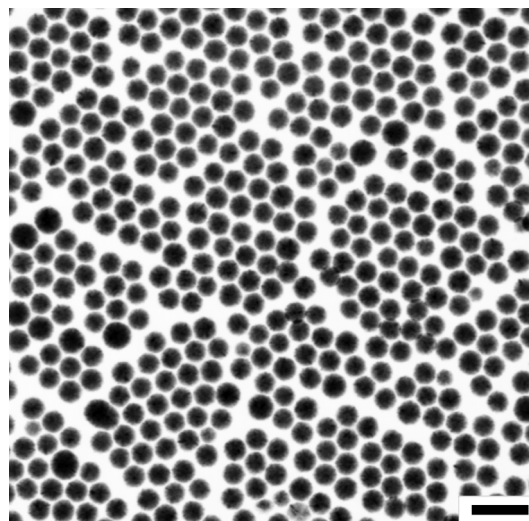


Figure 2. A TEM micrograph of ZnS–SiO₂ composite cores (sample 56SN–S1), radius $R = 84$ nm ($\delta = 6\%$), obtained after deposition of silica inside the ZnS pores. The size and polydispersity were determined by TEM. The presence of silica was detected by light scattering through an increase in the effective refractive index. The scale bar is 400 nm.

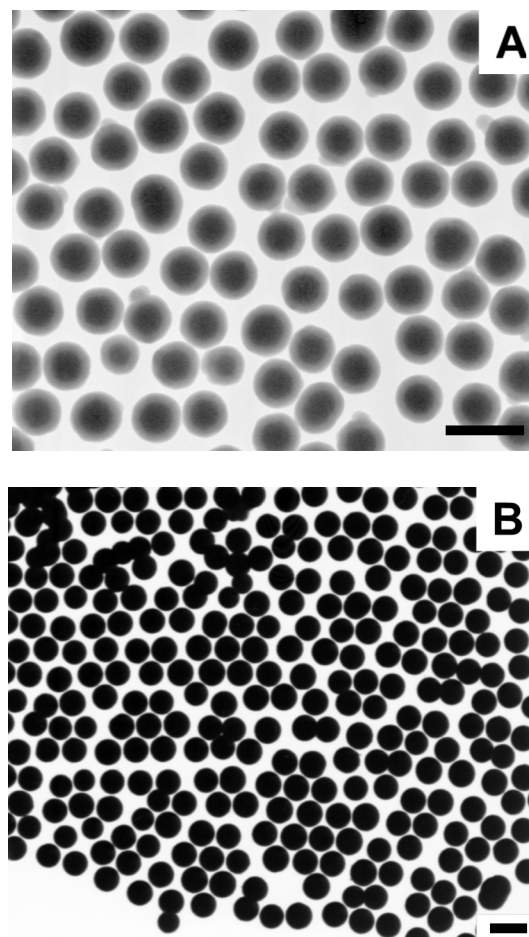


Figure 3. TEM micrographs of ZnS core–SiO₂ shell particles of different core-to-shell ratio and total size: (a) sample 56SN–S1–S, core radius $R_c = 84$ nm, total radius $R = 128$ nm, $\delta = 5\%$, scale bar 400 nm; (b) sample 54SN–S3, core radius $R_c = 346$ nm, total radius $R = 351$ nm, $\delta = 4\%$, scale bar 1 μ m. The size and polydispersity were determined by TEM.

concentration, the silica layer can be continuously grown to a desired thickness (Table 2). If the ZnS core radius is not too large (<200 nm using 100 keV), the silica shell can

(51) Duran, J. D. G.; Guindo, M. C.; Delgado, A. V.; Gonzalez-Caballero, F. *Langmuir* **1995**, *11*, 3648.

(52) Duran, J. D. G.; Guindo, M. C.; Delgado, A. V. *J. Colloid Interface Sci.* **1995**, *173*, 436.

(53) Toikka, G.; Hayes, R. A.; Ralston, J. *Langmuir* **1996**, *12*, 3783.

(54) Toikka, G.; Hayes, R. A.; Ralston, J. *Colloids Surf., A* **1998**, *141*, 3.

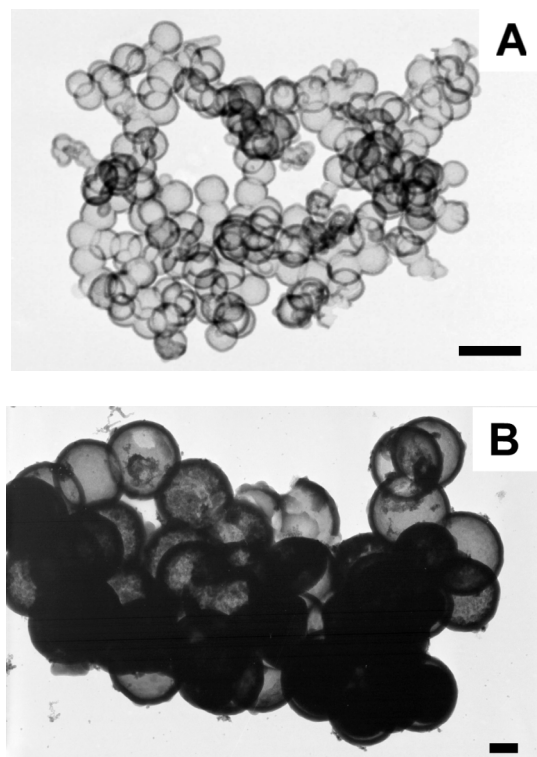


Figure 4. TEM micrographs of hollow silica shells obtained after dissolution of the ZnS cores: (a) shell thickness 17 nm with an internal radius of 60 nm; (b) shell thickness 50 nm with an internal radius of 260 nm. The scale bars are 200 nm.

be directly observed by TEM (Figure 3a) because not all electrons used in the imaging are stopped by the particle and there is an appreciable density difference between silica ($\sim 2.0 \text{ g/cm}^3$ ³⁴) and ZnS (4.0 g/cm^3 ⁵⁵). If the particles are larger than $\sim 200 \text{ nm}$, the silica shell can be discerned indirectly because the surface has become smoother (Figure 3b), by light scattering measurements, or after dissolving the ZnS cores.

SiO₂ Shells. The silica layer, created by the Stöber syntheses, is porous with a pore size about 3 \AA .⁵⁶ This size is sufficiently large to allow free diffusion of Zn^{2+} and S^{2-} ions across the silica layer. Using this fact, we successfully dissolved the ZnS core using a dilute solution of nitric acid to increase the solubility and obtained hollow silica particles. Figure 4 shows a collection of hollow silica shell particles. The ZnS cores were removed by dissolution with 0.001 M HNO_3 in a water–ethanol mixture. Acid solutions with $\text{pH} > 3$ should be used to prevent aggregation of the silica shells. The ZnS core is accessible to the acid ions even through a $\sim 50 \text{ nm}$ thick silica layer (Figure 4b). The thickness of the silica layer of empty shells can be measured directly by TEM after dissolution of the ZnS core. Dissolution of the ZnS from a small ZnS–silica composite sphere led to a silica replica of the porous structure of the initial particle (Figure 5). These replicas represent the internal structure of the ZnS core showing that ZnS particles are indeed porous.¹⁸ Silica shells have interesting optical properties on a single particle level and can also be used to create dielectric defects⁵⁷ if incorporated in a colloidal crystal of core–shell or homogeneous particles.

(55) David, R. L. *Handbook of chemistry and physics*, 76th ed.; CRC Press: Boca Raton, FL, 1995–1996.

(56) Walcarius, A.; Despas, C.; Bessiere, J. *Microporous Mesoporous Mater.* **1998**, *23*, 309.

(57) Pradhan, R. D.; Tarhan, I. I.; Watson, G. H. *Phys. Rev. B: Condens. Matter* **1996**, *54*, 13721.

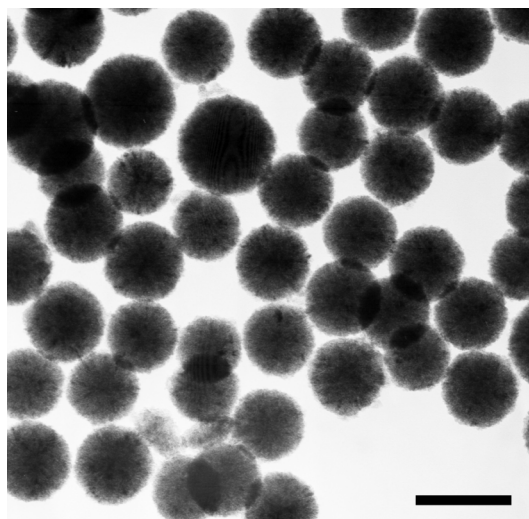


Figure 5. TEM micrographs of silica replicas obtained after dissolution of the ZnS from the ZnS–SiO₂ composite cores (sample 50SN-S1). The internal morphology of the pores can be seen inside the silica structure. The scale bar is 200 nm.

SiO₂ Core–ZnS Shell. It has been demonstrated that ZnS can be grown onto silica particles under similar conditions as ZnS cores by using H_2S ⁵⁸ or by sonification of a TAA solution.⁵⁹ In our experiments, we employed the thermal decomposition of TAA in an acidic water–ethanol mixture as a source of sulfide ions. Despite the fact that a low concentration ($< 0.001 \text{ M}$) of nitric acid was used to prevent aggregation of the suspension of SiO₂ seeds, the stability remained a problem. In all samples, a partial aggregation was found. Initially, ZnS forms irregularly shaped clusters composed of single nanocrystal crystals ($\sim 1\text{--}5 \text{ nm}$) on the silica surface (Figure 6a). The aggregates are held together by an irregular porous network. These clusters grow further and form a complete shell of dense ZnS. Figure 6b shows homogeneously coated core–shell particles. From broken ZnS shells, the thickness of the ZnS layer was estimated to be $\sim 50 \text{ nm}$. By showing the ability of growing both core–shell systems, we have control over the optical properties on a single particle level. These particles can be used to dielectrically dope photonic crystals⁵⁷ or grow inverse crystals from the shells.

ZnS Shells. Solvent-filled ZnS shells were obtained after dissolving the SiO₂ cores using hydrofluoric acid. Surprisingly, the ZnS shell did not dissolve or dissolved much slower than silica in ethanol solution of HF and remained as hollow shells. Figure 7 shows TEM micrographs of hollow ZnS shells. In a comparison of the ZnS shell before and after dissolving the SiO₂, it can be seen that the surface is smoother than in the case of the SiO₂ core–ZnS shell particle. This is an indication of a partial dissolution of the ZnS. However, an optimal dissolution time was not determined.

High dielectric hollow particles, such as ZnS shells, have interesting optical properties.^{10,11} Until now, almost all inverse dielectric structures, that is, low dielectric spheres in an fcc arrangement in a high dielectric background, have been made by templating on an already formed crystal.⁶⁰ With our method, individual hollow spheres are generated which can subsequently be crystallized. Starting with individual shells gives more flexibility, however, if

(58) Dekany, I.; Turi, L.; Tombacz, E.; Fendler, J. H. *Langmuir* **1995**, *11*, 2285.

(59) Dhas, N. A.; Zaban, A.; Gedanken, A. *Chem. Mater.* **1999**, *11*, 806.

(60) Velev, O. D.; Kaler, E. W. *Adv. Mater.* **2000**, *12*, 531.

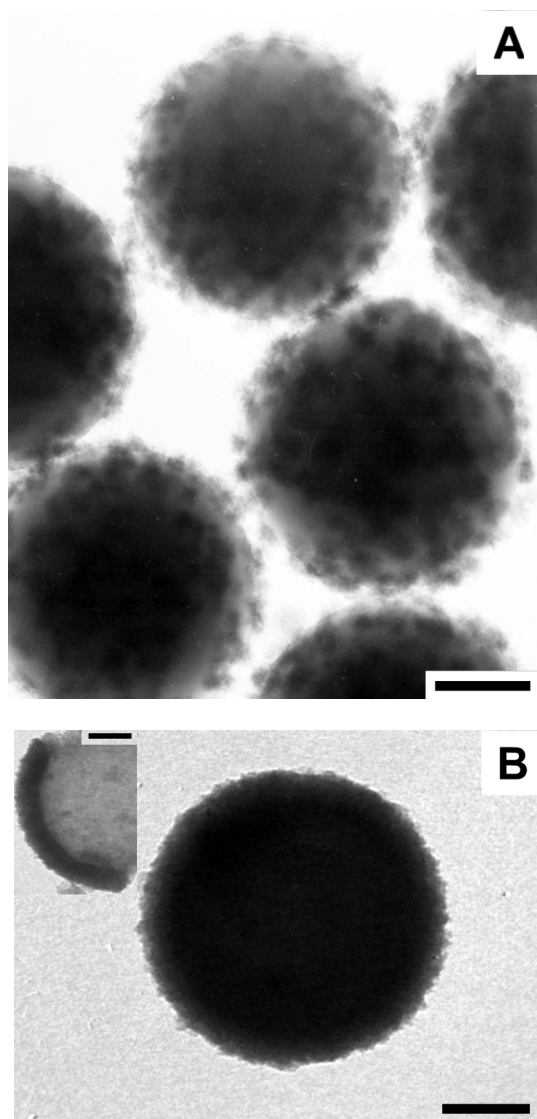


Figure 6. TEM micrographs of SiO₂ core–ZnS shell particles: (a) silica cores of radius 160 nm covered with an incomplete layer of ZnS nanocrystalline aggregates; (b) homogeneously coated silica seeds with a dense ZnS layer of thickness ~50 nm. The inset shows a broken ZnS shell. All scale bars are 100 nm.

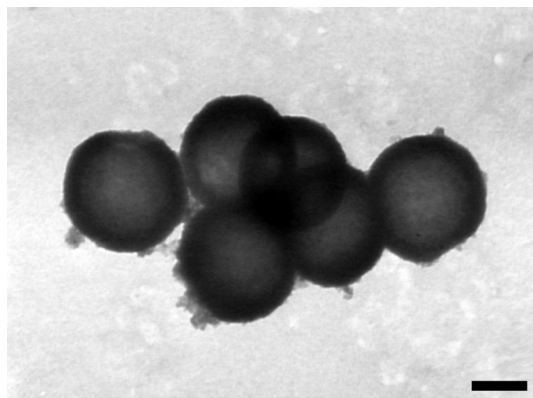


Figure 7. TEM micrographs of hollow ZnS shells obtained after dissolution of the silica cores by HF. The shell thickness is 50 nm with an internal radius of 160 nm. The scale bar is 200 nm.

one wants to dope the lattice dielectrically or wants to grow more complex lattices, like body centered tetragonal⁶¹ or binary lattices.⁶²

Optical Properties. Because of the high refractive index of β -ZnS ($n = 2.36^{26}$ at $\lambda = 589$ nm) and the size of the particles studied, a full solution of the Maxwell equations is necessary to quantitatively describe the light scattering of this system. Aden and Kerker derived an analytical solution for spherical core–shell particles.⁶³ The exact shape of the curves is sensitive to polydispersity, dielectric contrast, and particle size. We performed both wavelength-dependent (extinction) and angle-dependent (SLS) measurements on ZnS and ZnS core–SiO₂ particles only. The combination of both techniques gives a consistency check on the dielectric properties and structure obtained on the single particle level. All spectra were taken in the range above the absorption edge of bulk ZnS (350 nm).¹⁸

The extinction efficiency spectra and SLS spectra were calculated using scattering theory extended to the case of polydisperse particles assuming a Gaussian size distribution. In the case of core–shell particles, a Gaussian distribution was assumed in the core and an independent Gaussian distribution was assumed in the total particle radius.⁶⁴ Both distributions were measured by electron microscopy. The porous ZnS core cannot be represented with the refractive index of pure ZnS and requires a model. Fortunately, the ZnS nanocrystals are much smaller than the wavelength of light allowing a description of the particle by an effective dielectric constant of ZnS dispersed in a host of the solvent (or silica in the case of a composite ZnS–SiO₂ core). The effective dielectric constant was calculated using the Maxwell–Garnett effective medium approximation⁴⁶

$$\frac{\epsilon_{\text{eff}} - \epsilon_s}{\epsilon_{\text{eff}} + 2\epsilon_s} = f \frac{\epsilon_{\text{ZnS}} - \epsilon_s}{\epsilon_{\text{ZnS}} + 2\epsilon_s}$$

where f is the filling fraction of ZnS with a wavelength-dependent bulk dielectric constant ϵ_{ZnS} .²⁶ The particle pores are filled with a second material (solvent or silica in the case of the ZnS–SiO₂ composite core) with a dielectric constant ϵ_s . For the refractive index of silica ($n = 1.450$) and the solvent (ethanol $n = 1.361$), the wavelength dependence can be neglected. The most important fitting parameter obtained from the light scattering curves is the filling fraction of ZnS. Both the particle radii and polydispersity were varied as well, but the values taken were close to those determined from the electron microscopy.

In Figure 8, experimental and calculated extinction efficiency spectra of ZnS cores and the same cores coated with a ~44 nm silica shell are shown. The best fit was determined with an accuracy of ± 0.01 in the filling fraction of ZnS (± 0.01 in the refractive index) and ± 2 nm in the radius. In the case of core–shell particles, the core parameters were assumed to be the same and only the shell thickness was varied. A strong modulation of the scattering efficiency with wavelength, because of Mie resonances, was observed in large ZnS particles (Figure 9). The whispering gallery modes of the morphology-dependent resonances, averaged out in Figure 9a, can be observed only at low size polydispersity (Figure 9b). In general, the filling fraction of ZnS was determined to be in range of $f = 0.60$ – 0.80 , which is in good agreement with previous results.¹⁸ Angle resolved scattering (SLS)

(61) Dassanayake, U.; Fraden, S.; van Blaaderen, A. *J. Chem. Phys.* **2000**, *112*, 3851.

(62) Pusey, P. N.; Poon, W. C. K.; Ilett, S. M.; Bartlett, P. *J. Phys.: Condens. Matter* **1994**, *6*, A29.

(63) Aden, A. L.; Kerker, M. *J. Appl. Phys.* **1951**, 1242.

(64) Quirantes, A.; Delgado, A. V. *J. Phys. D: Appl. Phys.* **1997**, 2123.

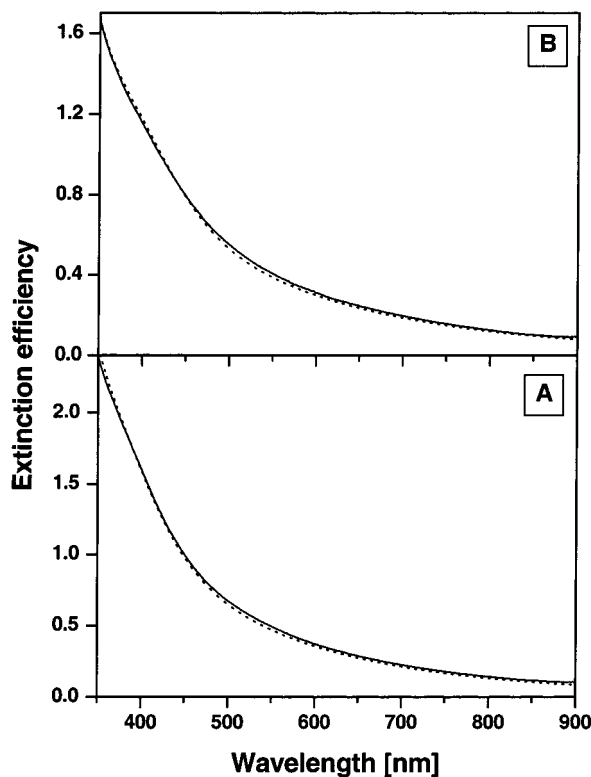


Figure 8. Experimental (solid line) and calculated (dotted line) extinction efficiency spectra: (a) ZnS cores (sample 56SN) of radius $R_c = 84$ nm, $\delta_c = 6\%$ (from TEM); (b) ZnS core-SiO₂ shell particles (sample 56SN-S1-S, Figure 3a), consisting of the same ZnS core, with total radius $R = 128$ nm, $\delta = 5\%$ (from TEM). The extinction efficiency spectra were calculated using the following parameters: $R_c = 92$ nm, $\delta_c = 5\%$, $R = 128$ nm, and $\delta = 5\%$. The filling fraction of ZnS in both cases is 0.62 ($n_{\text{eff}} = 1.92$ at $\lambda = 589$ nm).

curves (Figure 10) were in agreement with the extinction curves (Figure 9a) and showed no indication of particle aggregation.

For both SLS and extinction efficiency spectra, good agreement with Mie scattering theory was found for ZnS particles (cores) up to ~ 300 nm in radius. However, in the case of larger ZnS particles a good fit could not be obtained, probably because of an inhomogeneous distribution of ZnS in the particles (Figure 9b). The extinction curves of the smaller ZnS cores (Figure 8a) are not sensitive to an inhomogeneous distribution of ZnS. This is understandable, as the inhomogeneities have to be smaller than the wavelength. To give an idea of the effect of inhomogeneities for larger particles, we calculated a curve (Figure 9a) for a ZnS core with a radius of 350 nm in which the most simple inhomogeneous distribution, that of a core-shell, was assumed. Arbitrarily, we chose the core to have a radius of 200 nm with a filling fraction of 0.49 and the outer shell of 150 nm to have a filling fraction of 0.60. These values give a volume-averaged filling fraction that is the same (0.58) as that obtained from fitting the ZnS cores assuming a homogeneous particle. The curve calculated for a homogeneous distribution is closer to the measured values but is also not a perfect fit. The differences in both calculated curves make it clear that small inhomogeneities cannot be excluded. However, as no exact model is available for the radial dependence of the refractive index, we did not refine our calculations, as obtaining this function from scattering is an ill-defined problem.⁴⁶ The optical properties of the core-shell particles can be tuned by changing the thickness of the SiO₂

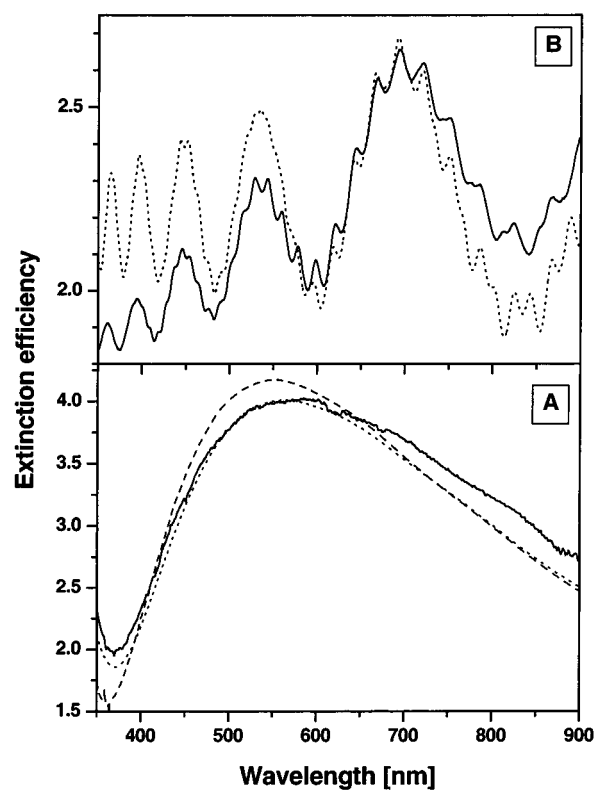


Figure 9. Experimental (solid line) and calculated (dotted line) extinction efficiency spectra: (a) ZnS particles (sample 54SN) of radius 346 nm and $\delta = 6\%$ (from TEM). The extinction efficiency spectra were calculated using the following parameters: $R = 350$ nm, $\delta = 6\%$, and ZnS filling fraction of $f = 0.58$ ($n_{\text{eff}} = 1.88$ at $\lambda = 589$ nm). The dashed line represents the calculated extinction efficiency of pure ZnS particles of total radius of 350 nm ($\delta = 6\%$) assuming a low-dense core ($R_c = 200$ nm, $f_c = 0.49$, $\delta_c = 6\%$) and a high-dense shell ($f_s = 0.49$) with a volume averaged filling fraction of 0.58; (b) highly modulated scattering by large monodisperse ZnS particles (see Figure 1b). The theoretical curve (dotted line) was calculated using $R = 1450$ nm, $f = 0.72$, and $\delta = 0.5\%$.

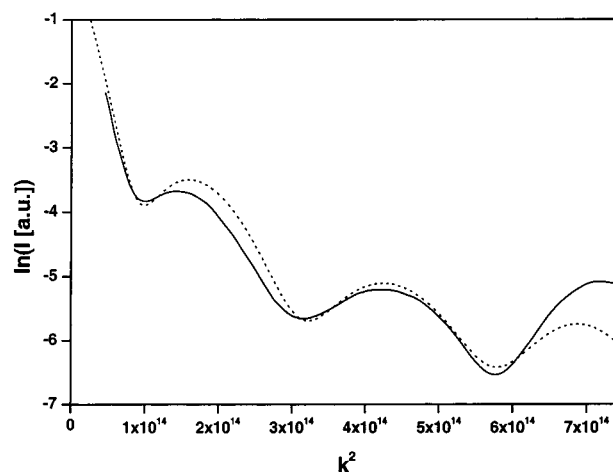


Figure 10. Experimental SLS spectra (solid line) of ZnS particles (sample 54SN) measured at $\lambda = 546$ nm. The theoretical curve (dotted line) was calculated using the same parameters (with $n_{\text{eff}} = 1.89$) as for the extinction efficiency spectra (Figure 9a).

(ZnS) shell with respect to the core radius. This is an important property, which can be employed to control the filling fraction of the high dielectric material in a photonic crystal made from colloidal crystal of core-shell particles.⁶⁵

Conclusions

We demonstrated that ZnS colloids covering most of the colloidal size range can be directly coated with a SiO₂ layer or vice versa to produce well-defined monodisperse core-shell particles. The coating procedure is performed without using a coupling agent and should be applicable to a variety of metal sulfides. The method produces monodisperse core-shell particles with a tunable core-to-shell size ratio and total radius. Both the ZnS and SiO₂ cores can be dissolved to produce hollow silica and ZnS shells, respectively. The optical properties of small ($R < 300$ nm) ZnS cores and ZnS core-SiO₂ shell particles are well described by an effective refractive index for the ZnS core. Larger ZnS particles cannot be described well as

homogeneous scatters. Because of the monodispersity and the high refractive index of the ZnS core (shell) and the availability of many coating procedures, the particles are ideal optical tracers, for instance, in light scattering⁶⁶ or optical tweezers studies,⁸ and are suitable building blocks for photonic crystals.¹³

Acknowledgment. We thank C. M. van Kats, A. Imhof (Utrecht University), and J. P. Hoogenboom (FOM AMOLF) for helpful discussions. This work is part of the research program of the Stichting voor Onderzoek der Materie, which is financially supported by the Nederlandse Organisatie voor Wetenschappelijk Onderzoek.

LA0101548

(65) Velikov, K. P.; Moroz, A.; van Blaaderen, A. Under preparation.

(66) Underwood, S. M.; van Megen, W. *Colloid Polym. Sci.* **1996**, *274*, 1072.